Proc. Natl. Acad. Sci. USA
Vol. 89, pp. 2409–2413, March 1992
Microbiology

Three-dimensional structure of Theiler murine encephalomyelitis virus (BeAn strain)

(picornavirus/x-ray crystallography/molecular replacement/neurovirulence)

MING LUO*†‡, CUNHENG HE*†, KENNETH S. TOTH*†, CARL X. ZHANG*, AND HOWARD L. LIPTON§

*Department of Microbiology, †Center for Macromolecular Crystallography, University of Alabama, Birmingham, AL 35294; and §Health Science Center, University of Colorado, Denver, CO 80262

Communicated by Michael G. Rossman, November 18, 1991 (received for review August 28, 1991)

ABSTRACT **Depending on the strain, Theiler murine encephalomyelitis virus (TMEV) may cause acute encephalitis or chronic demyelinating disease, which is associated with viral persistence in mice. Persistent central nervous system infection and demyelination by the less-virulent TMEV has provided a useful animal model for the human demyelinating disease multiple sclerosis. The less-virulent BeAn strain of TMEV was crystallized and its atomic structure was determined by x-ray crystallography. The α-carbon coordinates of the closely related Mengo virus were used to calculate the initial phases to 3.5 Å resolution and the interpretable electron density map was produced by 10 cycles of 30-fold noncrystallographic molecular replacement averaging. The structure revealed a high degree of overall structural similarity to Mengo virus as well as substantial differences in the surface loops. These structural changes might be correlated with TMEV host-specific recognition, pH-related stability, and neurovirulence.**

Theiler murine encephalomyelitis virus (TMEV) belongs to the family Picornaviridae. Although TMEV is currently classified as an enterovirus, nucleotide sequences suggest that TMEV should be classified as a member of the cardiovirus genus, which includes encephalomyocarditis virus and Mengo virus (1). The virion consists of a spherical protein shell that encapsidates a single-stranded RNA genome of positive polarity and 8098 nucleotides. There are four polypeptide species in the capsid, VP1 (37 kDa), VP2 (34 kDa), VP3 (27 kDa), and VP4 (6 kDa). The capsid presents an icosahedral symmetry and contains 60 copies of each of the four polypeptides. TMEV has been divided into two groups, the virulent group and the TO (Theiler's original) group (2). The first group consists of two highly virulent viruses, GDVII and FA, which cause a rapidly fatal encephalitis in mice. The second group includes all the remaining strains that resemble TO isolates. Members of the TO group are much less virulent than GDVII and FA but produce a biphasic central nervous system disease: acute poliomyelitis (early onset) followed by a chronic, inflammatory, demyelinating disease (late onset) associated with viral persistence. Persistent TMEV infection and demyelination in mice has provided a useful experimental animal model for the human demyelinating disease multiple sclerosis (3).

The three-dimensional structures of several picornaviruses have been determined by x-ray crystallography, including human rhinovirus 14 (HRV-14) (4), poliovirus (5), Mengo virus (6), and foot-and-mouth disease virus (FMDV) (7). In the studies of HRV-14, some interesting features were observed in the viral capsid. Except for VP4, which is a short internal polypeptide exposed to the RNA, all three major capsid proteins, VP1, VP2, and VP3, contain an eight-stranded antiparallel β-barrel folding motif, which exists in the capsids of many spherical viruses, ranging from RNA viruses to DNA viruses and from animal viruses to plant viruses. This indicates that these spherical viruses might have evolved from a common ancestor that used the β-barrel folding motif to construct the icosahedral capsid. On the exterior surface, the neutralizing immunogenic sites identified by sequencing antibody-selected escape mutants were located on protrusions on the rims of a deep depression (termed the canyon) surrounding the fivefold icosahedral axes. The canyon was hypothesized to be the receptor binding site based on the notion that the virus could escape neutralization by host antibodies by changing the amino acid structures in the protrusions while keeping a conserved receptor binding site hidden at the bottom of the canyon.

In structural studies of other picornaviruses, conformational changes of the viral capsid proteins were found to be associated with the binding of the virion to the host receptor. When Mengo virus was crystallized in 0.1 M phosphate buffer (pH 7.4), there was a disordered loop of seven amino acids of VP3 in the middle of a depressed region (the pit) (6). Under such conditions, the virions were unable to attach to the host receptor. If the crystallization buffer was changed to pH 4.6 or to a higher concentration of salt, the flexible loop assumed a rigid conformation approaching the FMDV (GH) loop of VP1 and virions could attach to the host receptor (8). Conformational changes were also observed in the structure of a chimeric poliovirus, constructed by substitution of the VP1 BC loop of the type 1 Mahoney strain with that of the type 2 Lansing strain (9). This substitution, which changed the host specificity of the Mahoney strain from primate to mouse cells, was accompanied by swelling of the entire VP1 pentamer array around the fivefold axes.

In this paper, we report the atomic structure of the BeAn strain of TMEV.¶ Since it has been shown that TMEV neurovirulence is related to the capsid proteins of different virus strains (10–12), this result might help in understanding host receptor recognition, pH-related stability, and neurovirulence.

MATERIALS AND METHODS

BeAn virus was propagated in BHK-21 cells and purified as described by Rozhon *et al.* (13). Several crystalline forms were obtained by the hanging drop vapor diffusion method and the tetragonal form, which was grown with PEG 3350 in 0.02 M boric acid buffer (pH 8.5), was suitable for x-ray diffraction structure analysis (14). Diffraction data were collected at the Cornell high-energy synchrotron station. The

The publication costs of this article were defrayed in part by page charge payment. This article must therefore be hereby marked "*advertisement*" in accordance with 18 U.S.C. §1734 solely to indicate this fact.

Abbreviations: TMEV, Theiler murine encephalomyelitis virus; HRV-14, human rhinovirus 14; FMDV, foot-and-mouth disease virus.

‡To whom reprint requests should be addressed.

¶The atomic coordinates and structure factors have been deposited in the Protein Data Bank, Chemistry Department, Brookhaven National Laboratory, Upton, NY 11973.

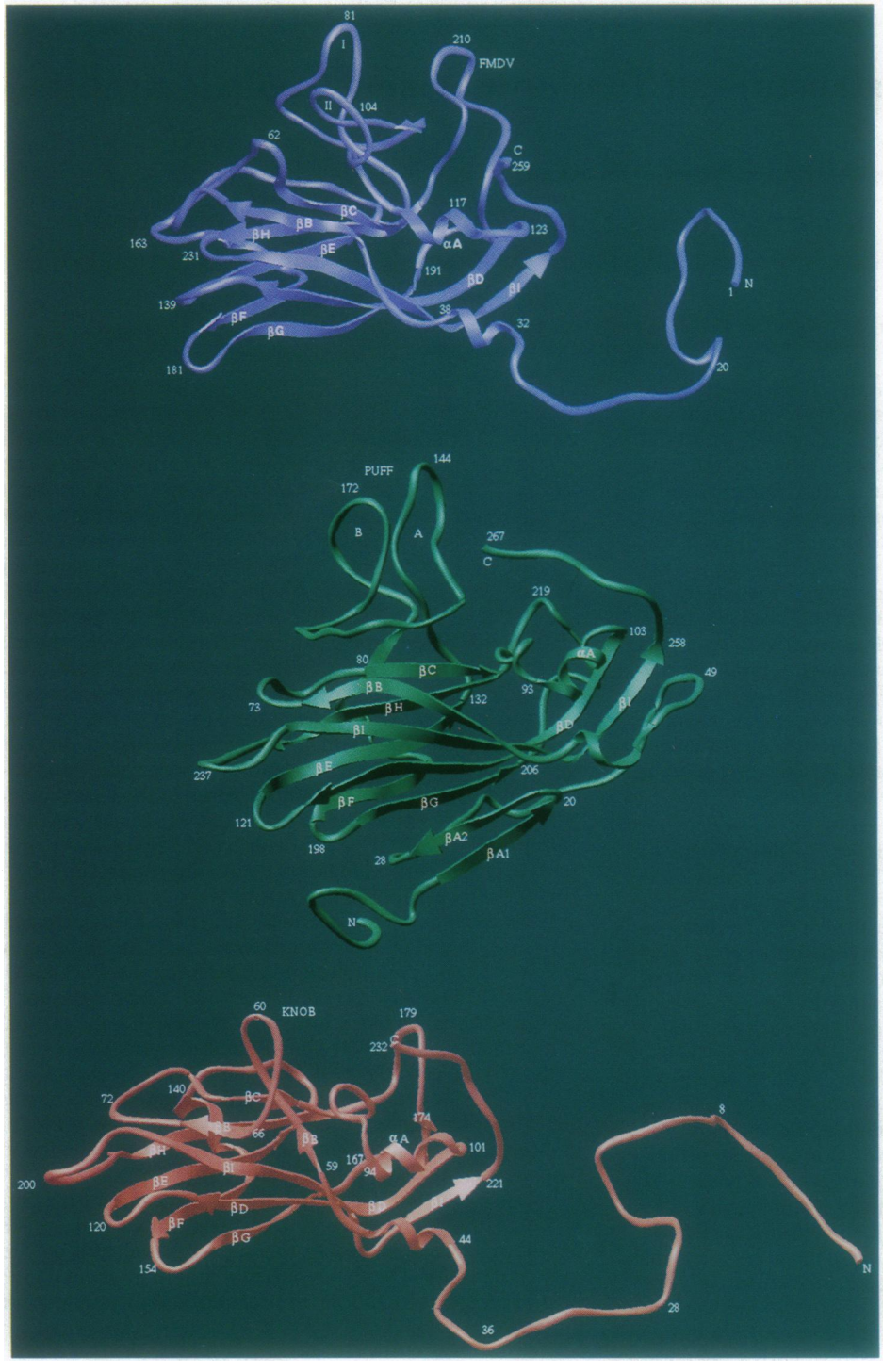

FIG. 1. Ribbon drawings of the three major capsid proteins, VP1, VP2, and VP3, in TMEV. Each major polypeptide contains the common β-barrel motif found in many spherical viruses. The nomenclature describing the secondary elements is the same as in Mengo virus. VP1 is blue, VP2 is green, and VP3 is red. The drawings were made with the program RIBBONS (by Mike Carson, University of Alabama at Birmingham).

unit cell was determined as tetragonal ($a = b = 331.86$ Å; $c = 796.26$ Å), and the Laue symmetry was 4/mm. The *R*sym was 13.1% for $I > 2\sigma$ and the final data set includes 209,592 unique reflections to 3 Å resolution (≈50% complete to 3.5 Å resolution). The pattern of systematic absence suggested that the space group should be $P4_122$ or $P4_322$. The crystallographic asymmetric unit contains half an icosahedral virus particle according to V_m calculations (2.5 for 4 particles per unit cell). The particle should sit on a crystallographic twofold axis and be located near (0.0, 0.5, 0.0) for packing considerations. A self-rotation function (using data between 5 and 15 Å resolution) (15) and a locked rotation function (using data between 10 and 30 Å resolution) (16) showed that the virus particle was rotated by 33.7° about the crystallographic twofold axis *b*, relative to the orientation of a chosen standard icosahedron (which has three twofold axes parallel to the orthogonal axes). An *R* factor search (7) using the α-carbon coordinates of Mengo virus and the data between 10 and 15 Å resolution selected the space group $P4_322$ and determined the precise particle location as (0.000, 0.510, 0.000). Initial phases were calculated to 3.5 Å resolution with the Mengo virus α-carbon coordinates and the electron density was averaged by 10 cycles over the thirtyfold noncrystallographic symmetry determined above. A spherical envelope of 170 Å outer radius and 80 Å inner radius was used during averaging (with tangent planes separating the overlapping regions) and Fc were substituted for the missing reflections starting at cycle 6. The overall correlation coefficient at cycle 10 was 0.72 and the *R* factor was 27.1% between Fo and Fc. The averaged electron density was

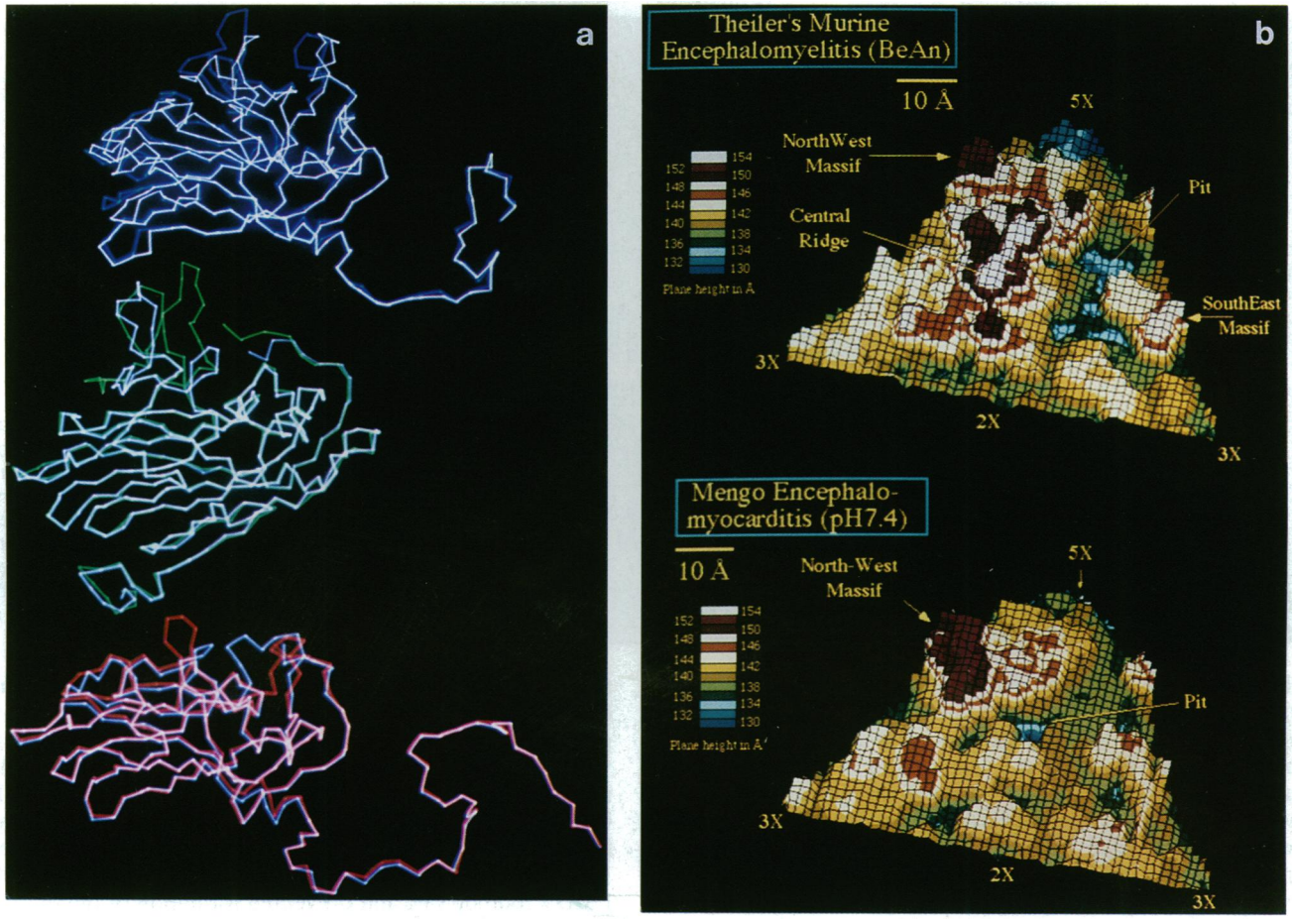

FIG. 2. (*a*) Superposition of α-carbon tracing of the major capsid proteins from TMEV and Mengo virus. Color code is the same as in Fig. 1. White lines are the polypeptide chains of Mengo virus. (*b*) Exterior topographic plot for TMEV and Mengo virus. There are extra protrusions on the TMEV surface labeled as the northwest massif, the central ridge, and the southeast massif. Pit area in TMEV has a different shape in comparison with Mengo virus.

viewed on a minimap and on the PS300 graphics computer with the FRODO program. Characteristic side chains could be easily identified and the polypeptide chain was traced within the icosahedral asymmetric unit. After building an atomic model, phases were calculated to 3.0 Å resolution (adding 16,000 more reflections) with the new complete atomic coordinates and the density was averaged for five more cycles.

RESULTS AND DISCUSSION

Structure Description. The three major capsid proteins, VP1, VP2, and VP3, have secondary structures similar to those of Mengo virus (Fig. 1). Each contains an eight-stranded antiparallel β-barrel motif, which has been found in all picornaviruses and most other spherical viruses studied to date (17). The nomenclature describing the Mengo virus structure is used here and the TMEV structure is compared with that of Mengo virus.

VP1. There are 276 residues in BeAn VP1 according to nucleotide sequencing (1), one amino acid less than the Mengo virus VP1. Most of the polypeptide chain has ordered electron density, the exception being the C-terminal residues 260–276. In Mengo virus, the C terminus of VP1 was also disordered beyond residue 260; however, weak density for residues 260–271 was later found in the refined structure (18). The Mengo virus C terminus was on the side of the pit (see Introduction) adjacent to the neighboring VP1. In TMEV, the orientation of Pro-259 suggested that the C terminus turns to the same direction. Loops I and II in TMEV are made up of residues 73–94 (residues 74–90 in Mengo virus) and 94–112 (residues 91–110 in Mengo virus), respectively. Loop I is larger in TMEV than in Mengo virus and is shifted toward the EF loop, while the top of loop II in TMEV is pointing more toward the fivefold axis. The extra five residues in loop I form a protrusion pointing up from the viral surface (Fig. 2*a*). There is also a three-amino acid deletion in the second corner (HI loop) relative to Mengo virus. This deletion leaves the third corner (DE loop) more exposed near the fivefold axis. Residues 211–215 in the FMDV loop are shifted toward the GH loop in VP3. There are additional minor conformational differences throughout the polypeptide chain, but the complete β-barrel motif and the N terminus can be superimposed on Mengo virus without any rotation or translation. A density was found on the fivefold axis at a radius of 120 Å that has height similar to that of the polypeptide region but cannot be counted for any amino acids. Similar densities found in HRV-14 and Mengo virus, which are located at radii of 157 and 140 Å, respectively, have been postulated as representing a bound metal ion (Ca^{2+} or Mg^{2+}). However, it is unlikely that the density in TMEV is a bound ion because there are no nearby amino acids that may act as suitable ligands. Finally, the hydrophobic core in the β-barrel is empty.

VP2. VP2 in TMEV (267 amino acids) is 11 residues longer than that in Mengo virus. This difference corresponds to an insertion in the first loop of the puff (the EF loop), which has a conformation similar to that of HRV-14. As a result, the puff in TMEV looks like a hybrid between HRV-14 and Mengo virus, the first loop (A) from HRV-14 and the second loop (B) from Mengo virus. The additional loop (A) in the TMEV puff has close interactions with the FMDV loop in VP1 (Fig. 2*a*),

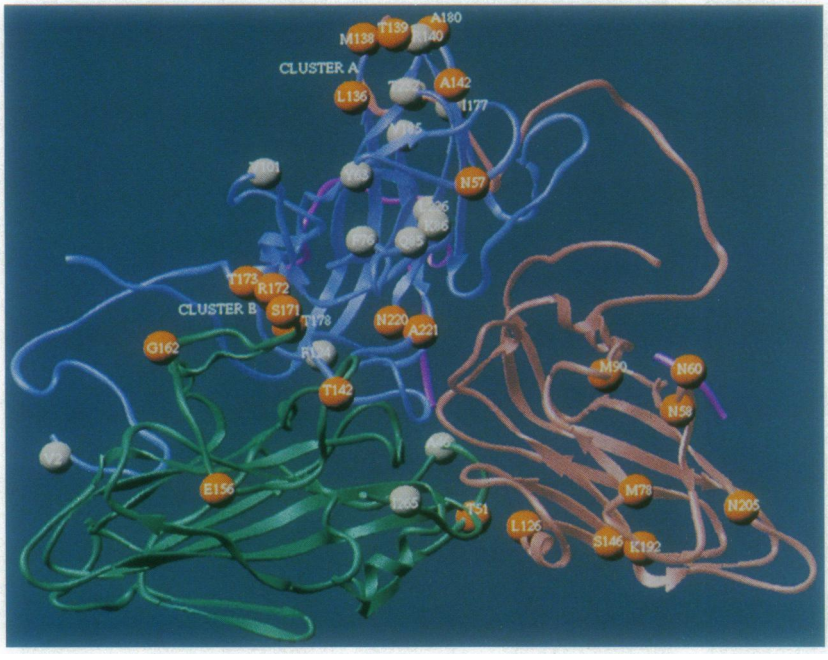

FIG. 3. An asymmetric unit of the icosahedral capsid is shown as a ribbon drawing. There is one copy of each capsid protein in the unit. Balls mark the BeAn residues in the major capsid proteins, which are different from GDVII. Conserved changes are light yellow; nonconserved changes are orange. Note the two clusters of nonconserved changes around the VP1 DE loop and the VP2 puff, respectively. The color code for the major VPs is the same as in Fig. 1 and the purple is for VP4.

which may give the virion extra stability (see below). The N termini are clearly visible and form an annulus around the threefold axis as seen in Mengo virus and FMDV. The conserved Ser-11, which was proposed to be involved in the autoproteolytic cleavage of VP0 in the mature virion (6), has the same side-chain orientation as in Mengo virus. However, experiments showed that Ser-10 of HRV-14 located at a similar position was not involved in the cleavage (19). The last three residues at the C terminus are shifted away from the twofold axis.

VP3. VP3 in TMEV has 232 amino acids (231 in Mengo virus) and has the most conserved structure compared to other picornaviruses. One conformational difference is seen on the tip of the knob (a loop inserted in βE) (Fig. 1). Residues 57–63 form a straight-ended loop pointing away from the pit. Another major difference occurs on the GH loop (residues 172–185) within the pit. The amino acid sequence of residues 176–182 in the loop is also highly variable among TMEV, Mengo virus, and HRV-14. This loop is completely ordered in TMEV but partially disordered in Mengo virus at pH 7.4. In Mengo virus, the loop changes its conformation according to pH and salt concentrations (8) (see below). There is also a slight main chain shift of TMEV relative to Mengo virus on the first corner (the BC loop). Cys-87 and Cys-89 do not form a disulfide bond as found in Mengo virus where Cys-86 and Cys-88 form a disulfide bond. The side-chain density suggests that the -SH group of Cys-89 is oxidized or has other modifications.

VP4. VP4 in TMEV (71 amino acids; 70 in Mengo virus) is largely disordered. Only two short segments of electron density are observed. The first segment near the fivefold axis corresponds to residues 13–37. This segment has the same conformation as that in Mengo virus. However, the positions of residues 13–15 at the N-terminal end suggest that the preceding segment of the VP4 N terminus is oriented in a different direction. The second segment is close to the C terminus of VP2 at the threefold axis. The sequence could not be clearly identified, but five amino acids may be fitted into the density.

Pit, the Putative Receptor Binding Site. The depression found in the contact region between VP1 and VP3 on the viral surface was designated as the pit when the structure of Mengo virus was determined. It was proposed as the putative receptor binding site based on its analogy to the canyon in HRV-14, and subsequent studies with Mengo virus indicated that the pit is indeed involved in the viral attachment to the host receptor (8). The GH loop of VP3 sits in the middle of the pit and was found disordered in the initial structure determination of Mengo virus using crystals grown in 0.1 M phosphate buffer (pH 7.4). Under these conditions, Mengo virus is not infectious and is unable to bind to its host cellular receptor. If the pH was reduced to 4.6, the GH loop in VP3 became ordered and assumed a conformation similar to that found in HRV-14, and the virus was then infectious. At pH 7.4, a phosphate molecule was bound at a site beneath the FMDV loop of VP1 and prevented formation of the ordered conformation of the GH loop; lowering the pH restored infectivity by removing the phosphate molecule in the presence of high concentrations of phosphate. The GH loop of TMEV VP3 is ordered even at pH 8.5 and assumes the same conformation as infectious Mengo virus (Fig. 2*a*). The potential phosphate binding site, similar to that in Mengo virus, still exists in TMEV, but the rigid conformation of the GH loop appears to block the entry of a phosphate molecule. Amino acid differences between BeAn and GDVII are located primarily outside of the pit (Fig. 3). It is known that BeAn and GDVII bind to the same receptor; therefore, the receptor binding site should be conserved between the two strains (20, 21). Moreover, the sequence variability of the TMEV GH loop from HRV-14 and Mengo virus also suggests its involvement in the host cellular receptor recognition.

pH-Related Stability. Although it has been suggested that TMEV should be classified in the cardiovirus genus, its stability under various pH values is different from other cardioviruses. A typical cardiovirus, such as encephalomyocarditis virus or Mengo virus, is destabilized around pH 6.2 by 0.15 M Cl^- or Br^- (22). Structural studies of Mengo virus showed that capsid stability was associated with the conformation of the FMDV loop in VP1 and the GH loop in VP3. At pH 6.2, the FMDV loop was more open than at pH 7.4, while the GH loop in VP3 keeps its disordered conformation. This leaves a large open space at the boundary between VP1 and VP3 in the pit. The virion at this conformation is unstable and starts to disassemble in the presence of 0.15 M Cl^- or Br^-. In case of TMEV, the GH loop has a rigid closed conformation even at pH 8.5. In addition, the first loop of the VP2 puff has extensive interactions with the FMDV loop, which may maintain the FMDV loop in its stable conformation (Fig. 2*a*). Residues Trp-202, Trp-206, and Phe-215 in VP1 have close interactions with Tyr-135 and Phe-151 in VP2, resulting in these five aromatic residues forming a semicircular hydrophobic core between the two loops. There is also

a hydrogen bond made by Glu-146 in VP2 to the NH group of Asp-214 in VP1. This stable conformation of the two TMEV surface loops may be responsible for the insensitivity of TMEV to pH changes (23). As a result, the uncoating of TMEV may be induced only by virion binding to the host receptor. The fact that FMDV is also unstable below pH 7.0 and that there are no loop interactions on the surface of FMDV supports this notion. The only loop present in FMDV is the highly mobile FMDV loop in VP1.

Neurovirulence and Persistent Infection. Efforts have been made to identify the sites on TMEV responsible for neurovirulence and persistent infection, which leads to demyelination. By constructing recombinant viruses between the highly virulent GDVII virus and the less virulent BeAn or DA viruses, determinants that attenuate neurovirulence were found in the 5′ noncoding region of the genomic RNA (10) and in sequences coding for the capsid proteins (10, 11). A site that allowed viral persistence and demyelination in mice was also located in the capsid region (12). These sites should map to the region where the amino acids are different in the two groups. The lethality of GDVII was lost when VP2 or VP1 of DA was substituted. However, the determinants for neurovirulence may not necessarily overlap with those resulting in viral persistence and demyelination (12). Fig. 3 displays the amino acids of BeAn virus, which are different from those of GDVII. It is clear that there are two clusters of nonconserved changes (orange spheres); cluster A is around the third corner of VP1,[‖] while cluster B is located on the second loop of the VP2 puff. Amino acids in these clusters are on surface loops accessible to antibodies. Cluster A on the third corner of VP1 is more exposed in TMEV than in Mengo virus and is partly equivalent to the neutralizing immunogenic site II in HRV-14 (4). Recently, Tang *et al.* (12) have shown that substitution of only VP1 from a less virulent DA strain into the virulent GDVII is sufficient to attenuate neurovirulence and allow viral persistence and demyelination in mice. Cluster A is the major site in VP1 that is hypervariable between DA and GDVII; therefore, it might be a T- or B-cell antigenic site differentiating the two strains. Early work has suggested that the mechanism of TMEV-induced demyelination involves host immune responses to the virus (24). Cluster B region has been indirectly shown to be a potential antigenic site and neurovirulence determinant (25). A single amino acid change (Thr-101 to Ile) on loop II of DA VP1 was identified in an antibody neutralization escape mutant, and this mutation was associated with a reduced ability of the virus to persist in the central nervous system (25). This amino acid is close to cluster B on the second loop of the VP2 puff, which forms a two-strand β-fold with loop II in VP1 via interactions of residues 94–96 in VP1 and residues 176–178 in VP2. The Thr-101 to Ile mutation on loop II of VP1 is likely to alter the interaction, which may result in conformational changes of the second loop of the VP2 puff. This would suggest that interactions between subunits via loops may have a direct effect on virus–host interactions and viral pathogenesis. Replacement of GDVII VP2 might loosen the critical interactions involving the VP2 puff and could lead to attenuation of GDVII neurovirulence.

[‖]The correct amino acid sequence for residues 138–140 in VP1 is Thr-Asp-Thr, which is corrected from the originally published sequence (Met-Thr-Arg) according to recent sequencing. Another correction is Gln-192 in VP3 (it was Lys in the original sequence).

TMEV vs. Mengo Virus. In general, the structures of TMEV capsid proteins are very similar to those of Mengo virus. The two virus structures could be superimposed on each other without any rotation or translation. The differences in main-chain conformation are found only on the exterior surface. Fig. 2 shows the main chain differences and the topographical differences on the viral surface. The changes in loops I and II of VP1, the puff of VP2, and the knob of VP3 make up the new topographical structural features in TMEV (named the northwest massif, the central ridge, and the southeast massif). The pit in TMEV appears to be different from the pit in Mengo virus. The pit is likely to be the site for receptor recognition. The surface loops probably contain the determinants of virion stability, neurovirulence of TMEV. The TMEV structure described here will allow design of experiments to identify the interactions of TMEV with its host.

We thank Lan Zhou, Janakiraman, Danrey W. Toth, and Kristi Jansen for help in data collection and virus preparation. We thank Drs. J. Y. Sgro and A. C. Palmenberg for making Fig. 2*b*. We also would like to thank Drs. M. G. Rossmann and J. E. Johnson for time on the Cyber 205 supercomputer. We are very grateful to Dr. Don Bilderback and the Cornell high-energy synchrotron source staff for their assistance on synchrotron data collection. The work is supported by a grant (P01 NS 23349-04) from the National Institutes of Health.

1. Pevear, D. C., Calenoff, M., Rozhon, E. & Lipton, H. L. (1987) *J. Virol.* **61**, 1507–1516.
2. Theiler, M. (1937) *J. Exp. Med.* **65**, 705–719.
3. Lipton, H. L., Miller, S. D., Melvold, R. M. & Fujinami, R. S. (1986) in *Concepts in Viral Pathogenesis. Vol. II*, eds. Notkins, & Oldstone, (Academic, New York), pp. 248–253.
4. Rossmann, M. G., Arnold, E., Erickson, J. W., Frankenberger, E. A., Griffith, J. P., Hetch, H. J., Johnson, J. E., Kamer, G., Luo, M., Mosser, A. G., Rueckert, R. R., Sherry, B. & Vriend, G. (1985) *Nature (London)* **317**, 145–153.
5. Hogle, J. M., Chow, M. & Filman, D. J. (1985) *Science* **229**, 1358–1365.
6. Luo, M., Vriend, G., Kamer, G., Minor, I., Arnold, E., Rossmann, M. G., Boege, U., Scraba, D. G., Duke, G. M. & Palmenberg, A. C. (1987) *Science* **235**, 182–191.
7. Acharya, R., Fry, E., Stuart, D., Fox, G., Rowlands, D. & Brown, F. (1989) *Nature (London)* **337**, 709–718.
8. Kim, S., Boege, U., Krishnaswamy, S., Minor, I., Smith, T. J., Luo, M., Scraba, D. G. & Rossmann, M. G. (1990) *Virology* **175**, 176–190.
9. Hogle, J. M., Syed, R., Fricks, C. E., Icenogle, J. P., Flore, O. & Filman, D. J. (1990) in *New Aspects of Positive-Strand RNA Viruses*, eds. Brinton, M. A. & Heinz, F. X. (ASM, Washington), p. 199.
10. Calenoff, M. A., Faaberg, K. S. & Lipton, H. L. (1990) *Proc. Natl. Acad. Sci. USA* **87**, 978–982.
11. Fu, J., Rodriguez, M. & Roos, R. P. (1990) *J. Virol.* **64**, 6345–6348.
12. Tangy, F., McAllister, A., Aubert, C. & Brahic, M. (1991) *J. Virol.* **65**, 1616–1618.
13. Rozhon, E. J., Lipton, H. L. & Brown, F. (1982) *J. Gen. Virol.* **61**, 157–165.
14. Luo, M., Zhang, C. X., Toth, D. W. & Lipton, H. L. (1992) *J. Cryst. Growth*, in press.
15. Rossmann, M. G. & Blow, D. M. (1962) *Acta Crystallogr. Sect. A* **15**, 24–31.
16. Tong, L. & Rossmann, M. G. (1991) *Acta Crystallogr. Sect. A* **46**, 783–792.
17. Rossmann, M. G. & Johnson, J. E. (1989) *Annu. Rev. Biochem.* **58**, 533–573.
18. Krishnaswamy, S. & Rossmann, M. G. (1990) *J. Mol. Biol.* **211**, 803–844.
19. Harber, J. J., Bradley, J., Anderson, C. W. & Wimmer, E. (1991) *J. Virol.* **65**, 326–334.
20. Kilpatrick, D. R. & Lipton, H. L. (1991) *J. Virol.* **65**, 5244–5249.
21. Fotiadis, C., Kilpatrick, D. R. & Lipton, H. J. (1991) *Virology* **182**, 565–570.
22. Dunker, A. K. & Rueckert, R. R. (1971) *J. Mol. Biol.* **58**, 217–235.
23. Speir, R. W., Aliminosa, K. V. & Southam, C. M. (1962) *Proc. Exp. Soc. Biol. Med.* **109**, 80–82.
24. Yamada, M., Zurbriggen, A. & Fujinami, R. S. (1991) *Adv. Virus Res.* **39**, 291–320.
25. Zurbriggen, A., Thomas, C., Yamada, M., Roos, R. P. & Fujinami, R. S. (1991) *J. Virol.* **65**, 1929–1937.